

# Selective Ethylene Oligomerization with Chromium Complexes Bearing Pyridine–Phosphine Ligands: Influence of Ligand Structure on Catalytic Behavior

Yun Yang,<sup>†,‡</sup> Joanna Gurnham,<sup>§</sup> Boping Liu,<sup>‡</sup> Robbert Duchateau,<sup>\*,†</sup> Sandro Gambarotta,<sup>\*,§</sup> and Ilia Korobkov<sup>||</sup>

<sup>†</sup>Department of Chemical Engineering and Chemistry, Eindhoven University of Technology, P.O. Box 513, Eindhoven 5600 MB, The Netherlands

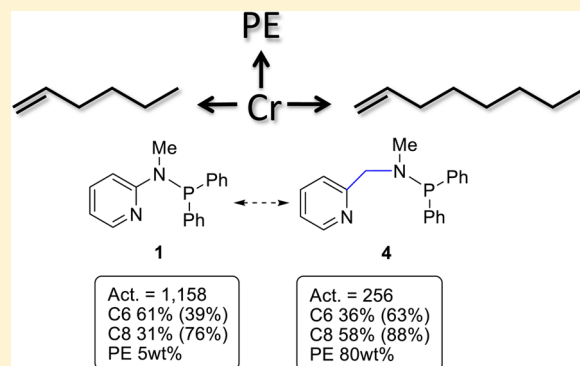
<sup>‡</sup>State Key Laboratory of Chemical Engineering, East China University of Science and Technology, Meilong Road 130, Shanghai 200237, China

<sup>§</sup>Department of Chemistry, University of Ottawa, Ottawa, Ontario K1N 6N5, Canada

<sup>||</sup>X-ray Core facility, Faculty of Science, University of Ottawa, Ottawa, Ontario K1N 6N5, Canada

## Supporting Information

**ABSTRACT:** Chromium complexes bearing a series of pyridine–phosphine ligands have been synthesized and examined for their catalytic behavior in ethylene oligomerization. The choice of solvent, toluene versus methylcyclohexane, shows a pronounced influence on the catalytic activity for all these complexes. Variations of the ligand system have been introduced by modifying the phosphine substituents affecting ligand bite angles and flexibility. It has been demonstrated that minor differences in the ligand structure can result in remarkable changes not only in catalytic activity but also in selectivity toward  $\alpha$ -olefins versus polyethylene and distribution of oligomeric products. Ligand  $\text{PyCH}_2\text{N}(\text{Me})\text{P}^i\text{Pr}_2$ , in combination with  $\text{CrCl}_3(\text{THF})_3$  afforded selective ethylene tri- and tetramerization, giving 1-hexene and 1-octene with good overall selectivity and high purity, albeit with the presence of small amounts of PE.



## INTRODUCTION

1-Hexene and 1-octene are utilized as comonomers for the production of linear low density polyethylene (LLDPE). Their rapidly growing market demand in recent years has stimulated research for finding new selective ethylene trimerization and tetramerization catalysts.<sup>1–6</sup>

The majority of the currently existing ethylene trimerization and tetramerization systems are based on chromium complexes bearing a wide variety of ancillary ligands.<sup>1,3,4</sup> As a result of ready interconversion between mono-, di-, and trivalent oxidation states of chromium, the same precursor might promote state-dependent selective or nonselective ethylene oligomerization as well as ethylene polymerization as a function of the reaction conditions (i.e., cocatalyst, solvent, temperature). This versatility in catalytic performance makes chromium catalysts excellent candidates for investigating factors that influence catalytic behavior.

The nature of the ancillary ligand also plays a fundamental role in determining the performance of the catalysts. In general, multidentate ligands containing P and N donors have a strong potential to facilitate the selective ethylene oligomerization affording 1-hexene with high selectivity but also the highly

desired 1-octene.<sup>7–23</sup> Typical examples are the BP Cr-PNP<sup>OMe</sup> trimerization system,<sup>8,24,25</sup> the Sasol Cr-PNP tetramerization system,<sup>9,26–28</sup> and the Cr-PNPN trimerization system developed by Rosenthal and co-workers.<sup>10,29–32</sup> The Cr-PNPN system recently reported by Gambarotta and co-workers was found to be capable of producing 91% 1-octene with 9% 1-hexene as the only side product, which reiterates the viability of P, N-based ligands to drive the reaction toward selective oligomerization.<sup>17</sup> Albeit in the absence of a P donor, chromium complexes bearing aminodipyridine ligands (Cr-NNN) afford pure 1-octene or 1-hexene, depending on the steric bulk of the ancillary ligand, alongside significant amounts of PE wax.<sup>33</sup> Similarly, removing the *ortho*-methoxy substituents from the phenyl group of Cr-PNP complexes shifted the catalytic selectivity from ethylene trimerization (ca. 90% 1-hexene) into tetramerization (up to 70% 1-octene).<sup>8,9</sup> Although it is not clear whether the switch in the C<sub>6</sub>/C<sub>8</sub> product ratio is

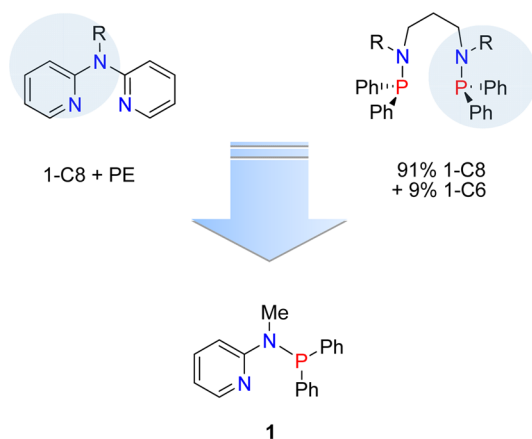
**Special Issue:** Catalytic and Organometallic Chemistry of Earth-Abundant Metals

**Received:** April 8, 2014

mediated by ligand sterics, coordination of the pendant methoxy group to chromium, or both,<sup>8,24,34,35</sup> this finding demonstrates that even subtle ligand modifications can significantly influence the catalytic behavior.

Given the versatility of the Cr-PNNP and Cr-NNN systems as catalysts for 1-octene production, in the present study, we have attempted to synthesize ligand **1**, which is assembled from fragments of both the PNNP and the aminodipyridine ligand (Scheme 1), hoping that it would provide high 1-octene

### Scheme 1. Design of Ligand 1



selectivity. To investigate the correlation between the catalytic performance and the ligand structure, the skeleton of ligand **1** was modified, giving a series of ligands with different phosphine moieties or P–Cr–N bite angles. The corresponding chromium adducts of the various ligands were activated with different cocatalysts and subsequently examined for their ethylene oligomerization behavior.

## RESULTS AND DISCUSSION

Ligand PyN(Me)PPh<sub>2</sub> (**1**) was readily prepared by the reaction of 2-(methylamino)pyridine and chlorodiphenylphosphine. Complexation of **1** with CrCl<sub>3</sub>(THF)<sub>3</sub> was conducted in dichloromethane, and the ligation was indicated by an instant color change from purple to blue upon mixing in dichloromethane. The resulting complex **1a** was isolated as a blue powder by removing the solvent *in vacuo*. Attempts to recrystallize complex **1a** from dichloromethane/petroleum ether resulted in microcrystalline material, unfortunately not

suitable for a single crystal X-ray diffraction analysis. Elemental analysis pointed to the postulated octahedral structure consisting of a chromium atom bonded by one ligand, one THF, and three chlorines: [PyN(Me)PPh<sub>2</sub>]CrCl<sub>3</sub>(THF) (**1a**). The proposed structure of **1a** is supported by the X-ray crystal structure determination of **2a** (*vide infra*).

Ethylene oligomerization reactions were carried out in methylcyclohexane using 500 equiv of methylaluminoxane (MAO) as activator. Since the catalytic behavior of complex **1a** and a mixture of CrCl<sub>3</sub>(THF)<sub>3</sub> plus ligand **1** in a 1:1 ratio were found to be identical, extensive oligomerization runs were conducted with *in situ* generated catalysts (Table 1). Upon activation, CrCl<sub>3</sub>(THF)<sub>3</sub>/**1** afforded fairly good activity, which is comparable to the highest activity reported in a similar chromium-catalyzed selective ethylene oligomerization system (1322 g/mmol Cr/h, 80 °C, 40 bar of ethylene).<sup>17</sup> C<sub>6</sub> and C<sub>8</sub> fractions predominated the liquid oligomeric products with an overall selectivity exceeding 90%. The remaining 10% of liquid products ranged from C<sub>10</sub> to higher oligomers, characteristic for a statistical product distribution. Besides oligomers, relatively small quantities (5 wt %) of polyethylene were also obtained. The simultaneous formation of mainly C<sub>6</sub>/C<sub>8</sub> oligomers and minor amounts of a statistical distribution of ≥C<sub>10</sub> oligomers and polyethylene suggests the presence of multiple active species possibly bearing chromium in different oxidation states.<sup>36,37</sup>

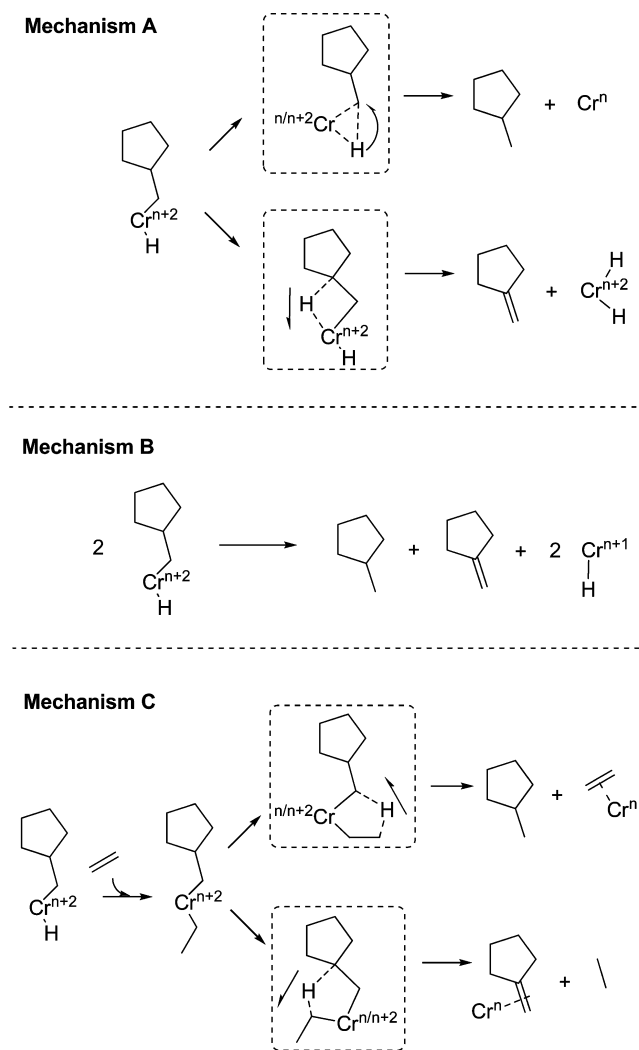
The purity of 1-hexene was found to be surprisingly low and over half of the C<sub>6</sub> fraction consisted of methylcyclopentane and methylenecyclopentane in a 1:1 ratio. These cyclic C<sub>6</sub> compounds are inferred to arise from a chromium cyclopentylmethyl hydride species, which is formed upon the rearrangement of the chromacycloheptane intermediate. This postulated mechanism was first proposed for their formation in the Sasol Cr-PNP ethylene tetramerization system, suggesting that the methylcyclopentane and methylenecyclopentane are produced by a reductive elimination and β-hydrogen transfer from the chromium cyclopentylmethyl hydride species, respectively (mechanism A, Scheme 2); or by disproportionation from two chromium cyclopentylmethyl hydride species (mechanism B, Scheme 2).<sup>38</sup> A recent DFT study by Budzelaar proved the accessibility of these cyclic C<sub>6</sub> products and proposed an alternative mechanism that the methylcyclopentane and methylenecyclopentane arise from an ethylene insertion into the Cr–H bond of chromium cyclopentylmethyl hydride species followed by hydrogen transfer to or from the

**Table 1. Ethylene Oligomerization Tests on Cr/Ligand 1<sup>a</sup>**

entry	cocatalyst (equiv)	PE (g)	PE (wt %)	LAO (mL)	activity (g/(mmol Cr·h))	C6 (1-C6) (%)	C8 (1-C8) (%)
1 <sup>b</sup>	MAO (500)	1.04	49	1.49	422	52.0 (62)	27.5 (77)
2	MAO (500)	0.26	5	7.18	1158	60.8 (39)	31.3 (76)
3 <sup>c</sup>	MAO (500)	0.56	10	7.04	1105	57.2 (40)	30.1 (73)
4 <sup>d</sup>	MAO (500)	1.38	14	12.43	2023	58.5 (44)	31.3 (73)
5	MMAO (500)	0.18	2	11.18	1612	60.4 (41)	30.3 (72)
6	DMAO (500)	0.47	14	4.23	685	63.3 (37)	29.0 (72)
7	DMAO (500)/TIBA (100)	0.18	3	8.32	1207	59.3 (39)	30.5 (70)
8 <sup>e</sup>	MAO (500)	0.18	53	0.21	66		
9 <sup>e</sup>	DMAO (500)/DEAC (50)	15.64	100	0	3127		
10 <sup>f</sup>	MAO (500)	0.37	56	0.40	132		
11 <sup>f</sup>	DMAO (500)/DEAC (50)	3.80	100	0	761		

<sup>a</sup>Conditions: CrCl<sub>3</sub>(THF)<sub>3</sub> = 10 μmol, ligand **1** = 10 μmol, methylcyclohexane=100 mL, 60 °C, 30 bar of ethylene, 30 min. <sup>b</sup>Toluene.

<sup>c</sup>CrCl<sub>3</sub>(THF)<sub>3</sub> = 10 μmol, ligand **1** = 20 μmol. <sup>d</sup>50 bar of ethylene. <sup>e</sup>Cr(acac)<sub>3</sub>·Cr(EH)<sub>3</sub>.

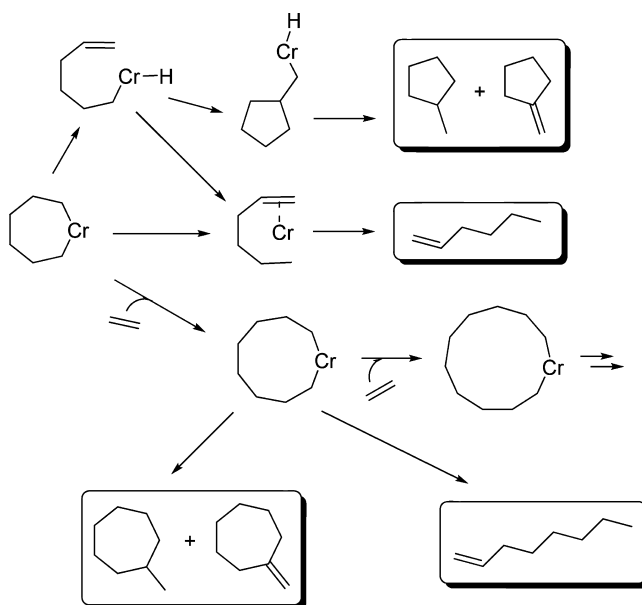
Scheme 2. Postulated Mechanisms A, B, and C for the Formation of Cyclic C<sub>6</sub> Products<sup>a</sup>

<sup>a</sup>Transition states are exhibited in the dotted rectangles.

chromium cyclopentylmethyl ethyl species to form the cyclic products (mechanism C, Scheme 2).<sup>39</sup> Given the rather low 1-hexene purity in our system, we speculate that at the stage of the chromacycloheptane, the rearrangement step affording the chromium cyclopentylmethyl hydride species should be very competitive to the formation of 1-hexene (either concerted or stepwise routes) and further ring growth (Scheme 3). Moreover, the main side products (around 30%) in the C<sub>8</sub> fraction detected in our system are two C<sub>8</sub> compounds in a 1:1 ratio, which are probably methylcycloheptane and methyl-encycloheptane (these have also been observed in the Sasol Cr-PNP ethylene tetramerization system<sup>38</sup>) generated in a similar mechanism as for the formation of cyclic C<sub>6</sub> products.

Subsequently, the influence of reaction conditions on the catalytic performance of the CrCl<sub>3</sub>(THF)<sub>3</sub>/1 system was investigated (Table 1). Toluene as solvent negatively affected the catalytic performance, leading to an activity that corresponds to approximately 40% of the original activity obtained in methylcyclohexane and a significant increase of PE formation. The retarding effect of toluene is possibly due to the formation of inert Cr(I)-η<sup>6</sup>-toluene complexes.<sup>40</sup> Although 1-hexene purity is enhanced in toluene, the actual 1-hexene

Scheme 3. Further Reaction Routes from Chromacycloheptane Species



selectivity does not improve much, due to a reduced overall C<sub>6</sub> selectivity. Increasing the ethylene pressure from 30 to 50 bar doubled the catalytic activity. The production of both polyethylene and oligomers increased under higher ethylene pressure, albeit that PE formation was influenced more strongly. On the other hand, the C<sub>6</sub>/C<sub>8</sub> ratio was unaffected.<sup>41,42</sup> Increasing the ligand/Cr ratio did not affect the catalytic behavior with respect to ethylene oligomerization; however, it doubled the amount of PE. Hence, the *in situ* generated catalytic active species for ethylene oligomerization is inferred to comprise chromium and ligand 1 in a 1:1 ratio.

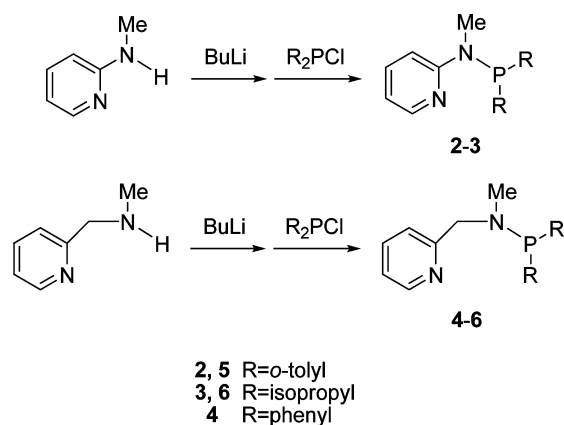
Changing the cocatalyst did not significantly influence the distribution of oligomers, implying the generation of identical active species for selective oligomerization. Varied weight percentages of PE indicate that the activation procedure affects the generation of the active species for oligomerization and polymerization to different extents. Modified MAO (MMAO) efficiently retards PE formation and drives the reaction toward oligomerization with improved activity, probably as a result of the better reducing capacity of MMAO compared with MAO. Using dried MAO (DMAO) as cocatalyst led to a drop in oligomer yield, which might be a result of insufficient reduction of the trivalent chromium precursor. Addition of triisobutylaluminum (TIBA) in DMAO gave results similar to MMAO in terms of inhibiting ethylene polymerization.<sup>43,44</sup>

Attempts to improve the catalytic activity for ethylene oligomerization by using more soluble chromium sources appeared to be unsuccessful. Upon activation with MAO, Cr(acac)<sub>3</sub>/1 only produced small amounts of oligomers and PE, which might imply that chlorine is needed to produce an active catalyst for selective ethylene oligomerization. Introduction of chlorine by using a combination of DMAO and diethylaluminum chloride (DEAC) as an alternative cocatalyst for Cr(acac)<sub>3</sub>/1, did restore the catalytic activity but unexpectedly shifted ethylene oligomerization toward ethylene polymerization. Given the absence of oligomeric products in the Cr(acac)<sub>3</sub>/1/MAO/DEAC system, the *in situ* generated active species is expected to differ from the one resulting from CrCl<sub>3</sub>(THF)<sub>3</sub>/1/MAO, although both combinations contain

chlorine. Using another chlorine-free compound,  $\text{Cr}(\text{EH})_3$  (chromium 2-ethylhexanoate), as the chromium precursor resulted in similar selectivity as that obtained for the  $\text{Cr}(\text{acac})_3/1/\text{MAO}/\text{DEAC}$  system but with a much lower ethylene polymerization activity.

In an attempt to improve the catalytic selectivity as well as to obtain insight into the factors affecting the catalytic behavior, ligand **1** was modified. Thus, a series of P,N-based ligands with varying substitutions on the phosphine moiety and different P–Cr–N bite angles has been synthesized (Scheme 4). Subsequently, the catalytic behavior of their corresponding *in situ*-prepared chromium complexes has been examined.

#### Scheme 4. Synthesis of Ligands 4–6



To investigate the steric and electronic effect determined by the phosphine moiety, the phenyl substituents on P in **1** were replaced by *o*-tolyl and isopropyl groups, affording ligands **2** and **3**, respectively. Their corresponding chromium complexes ( $[\text{PyN}(\text{Me})\text{PR}_2]\text{CrCl}_3\text{THF}$ ; R = *o*-tolyl (**2a**), isopropyl (**3a**)) were obtained from the reaction of **2** and **3** with  $\text{CrCl}_3(\text{THF})_3$  in THF. In the case of **2a**, crystals suitable for single crystal X-ray structure determination were grown by slow vapor diffusion of petroleum ether into a THF solution.

The crystal structure of **2a** (Figure 1) is in agreement with the earlier proposed structure of **1a** featuring a distorted octahedral geometry, in which the trivalent chromium is

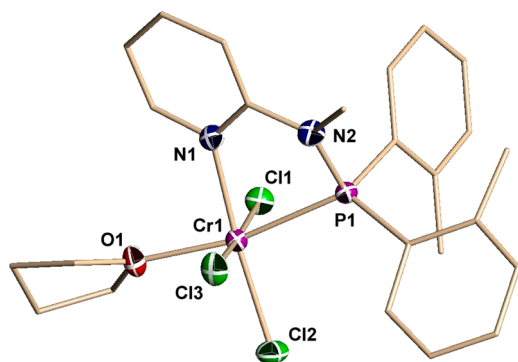


**Figure 1.** Partial thermal ellipsoid drawing of **2a** at 50% probability. Selected bond lengths (Å) and angles (deg): Cr1–P1 2.4298(6), Cr1–N1 2.0977(9), Cr1–Cl1 2.3019(8), Cr1–Cl2 2.3022(3), Cr1–Cl3 2.3086(2), Cr1–O1 2.0547(1); P1–Cr1–N1 75.84(35), O1–Cr1–N1 91.93(26), P1–Cr1–Cl2 99.42(5), P1–Cr1–O1 167.47(14), Cl2–Cr1–N1 175.03(29), Cl3–Cr1–Cl1 174.65(1).

chelated by the bidentate ligand **2** via the phosphine-P and the pyridine-N atoms. The distortion mainly arises from the acute P1–Cr1–N1 bite angle (76°). Chlorides and THF occupy the other four vacant sites in the octahedral coordinating sphere. The THF is located *trans* to the phosphorus donor. In an analogous octahedral complex  $[\text{Py}(\text{CH}_2)_2\text{N}(\text{Me})\text{PPh}_2]\text{CrCl}_3\text{THF}$ , the THF also resides *trans* to the phosphine functionality.<sup>18</sup> The *ortho*-methyl substitutions in the two *o*-tolyl groups are oriented opposite to each other. This might be attributed to steric factors as was revealed by DFT calculations (B3LYP/TZVP level) showing a 2.4 kcal/mol difference in energy between the most and least stable conformations.

A small change in the ligand structure by replacing the phenyl groups in the phosphine moiety with *o*-tolyl groups led to a remarkable change in catalytic behavior (Table 2, entries 1 and 2). The catalytic activity of **2a** in toluene was found to be 5-fold higher than that in methylcyclohexane, whereas **1a** is almost 3 times more active in methylcyclohexane than in toluene. The positive and negative effects of methylcyclohexane on the catalytic activity of **1a** and **2a** are confusing and possibly result from a combined contribution of solvent effects and a shift in the equilibrium of multiple active species. Interestingly, increased steric bulk on the phosphine moiety was found to give rise to improved purity of both 1-hexene and 1-octene.

Another interesting phenomenon observed for **2a** is the very long induction period for the reaction conducted in toluene. Unlike other chromium complexes in the present study, which invariably resulted in an instant exotherm after catalyst injection, **2a** consumes ethylene very slowly in the first 30 min of the reaction. The acceleration of ethylene uptake only starts when the temperature has reached a certain point (around 80 °C). Further conducted oligomerizations performed in toluene at varying temperatures using **2a** have revealed that this catalyst shows a strong dependence of its catalytic behavior on reaction temperature. Selective formation of C<sub>6</sub> and C<sub>8</sub> oligomers was only observed at elevated temperatures (Table 2, entries 1 and 4). However, when the reaction temperature of an uncontrolled reaction exceeded 105 °C, a rapid decay of the catalyst was indicated by the gradual decline of temperature. Reactions carried out under isothermal conditions (80 °C) led to nonselective oligomerization and higher percentages of PE, although a rather long catalyst lifetime was accomplished, with the rate of ethylene uptake remaining unchanged even after 150 min (Table 2, entry 3). Different catalytic outcomes under varying temperatures suggest that the active species responsible for PE formation is generated at a relatively low (≤80 °C) temperature, while the active species responsible for selective ethylene oligomerization is formed only at elevated temperature. A similar correlation between temperature and selectivity has also been reported for the Cr–NNN tetramerization system, in which 1-octene is only produced when the reactor temperature is uncontrolled and allowed to raise above 100 °C.<sup>33</sup>

Upon activation with MAO in toluene, **3a** also afforded C<sub>6</sub> and C<sub>8</sub> with good overall selectivity (Table 2, entries 5 and 6). Using methylcyclohexane as solvent led to a drop of activity and switched the selectivity slightly from C<sub>6</sub> to C<sub>8</sub>. In general, the oligomer distribution and reactivities of **2a** and **3a** show the same trend and differ from the catalytic behavior of **1a**. Compounds **2a** and **3a** both exhibit higher activity in toluene than in methylcyclohexane and an improved purity of short chain linear  $\alpha$ -olefins, although the purity is still far from being satisfactory. The fact that the catalytic behavior of **2a** resembles

Table 2. Ethylene Oligomerization Tests on 2a–6a<sup>a</sup>

entry	catalyst	solvent <sup>g</sup>	PE (g)	PE (wt %)	LAO (mL)	activity (g/(mmol Cr·h))	C <sub>6</sub> (1-C <sub>6</sub> ) (%)	C <sub>8</sub> (1-C <sub>8</sub> ) (%)
1 <sup>b</sup>	2a	toluene	1.68	9	23.47	2180	68.1 (92)	21.2 (85)
2	2a	MCH	0.26	12	2.62	415	68.1 (85)	27.6 (93)
3 <sup>c</sup>	2a	toluene	2.24	18	13.87	1660	38.7 (70)	16.3 (62)
4 <sup>d</sup>	2a	toluene	1.24	8	18.95	2945	77.8 (90)	12.5 (87)
5	3a	toluene	0.63	9	9.15	1394	65.5 (73)	31.9 (90)
6	3a	MCH	0.64	26	2.61	491	59.7 (68)	39.2 (90)
7	4a	toluene	2.19	20	12.12	2177	46.3 (>99)	31.0 (>99)
8	4a	MCH	1.03	80	0.36	256	35.5 (63)	57.9 (88)
9 <sup>e</sup>	4a	MCH	2.38	82	0.72	577	32.4 (59)	60.9 (93)
10 <sup>f</sup>	4a	MCH	0.40	53	0.48	150	23.2 (84)	52.7 (72)
11	5a	toluene	4.63	100		927		
12	5a	MCH	1.80	48	2.81	756	57.9 (95)	30.0 (65)
13	6a	toluene	0.96	70	0.58	276	50.7 (>99)	29.5 (>99)
14	6a	MCH	0.31	12	3.18	500	71.5 (98)	26.7 (>99)

<sup>a</sup>Reaction conditions: catalyst = 10 μmol, 500 equiv of MAO, solvent = 100 mL, 60 °C, ethylene (30 bar), 30 min. <sup>b</sup>50 min, 60–110 °C. <sup>c</sup>150 min, 80 °C. <sup>d</sup>80–110 °C. <sup>e</sup>50 bar. <sup>f</sup>500 equiv of DMAO and 50 equiv of TEA. <sup>g</sup>MCH = methylcyclohexane.

more than that of 3a, containing aliphatic isopropyl substitution on phosphorus, than that of 1a, containing aromatic phenyl groups, is puzzling and indicates that electronic effects can be ruled out.

For the PNP type of ligands, introduction of a CH<sub>2</sub> unit in one of the P–N bonds shifted the dominant oligomer fraction from 1-octene to 1-hexene, which shows that varying the ligand bite angle and flexibility might dramatically impact the product distribution.<sup>9,19</sup> Encouraged by this finding, introduction of a carbon linkage between the pyridine and the aminophosphine fragments was endeavored for 1–3, affording the analogous ligands 4–6 (Scheme 4). These ligands were then reacted with CrCl<sub>3</sub>(THF)<sub>3</sub> to afford corresponding chromium complexes. The crystals of 4a were suitable for X-ray diffraction analysis, and the results confirmed the anticipated ligand coordination (Figure 2). The crystal structure of 4a displays the typical

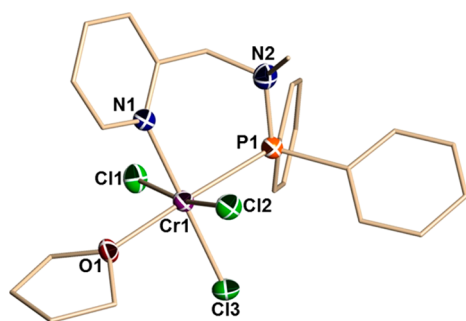


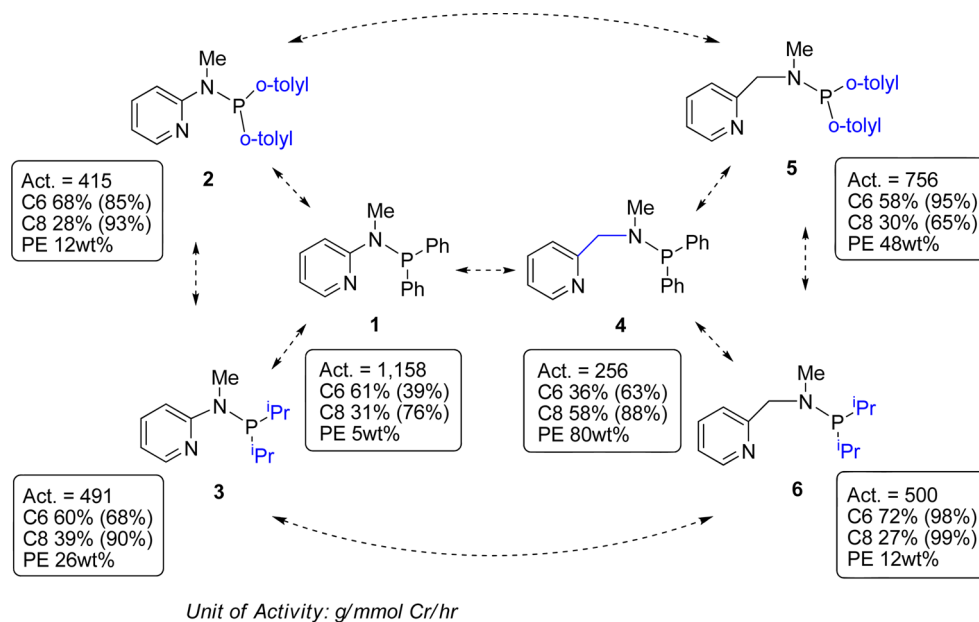
**Figure 2.** Drawing of 4a with thermal ellipsoids drawn at 50% probability. Select bond lengths (Å) and angles (deg) of 4a: Cr1–P1 2.432(2), Cr1–N1 2.164(6), Cr–Cl1 2.317(2), Cr1–Cl3 2.301(2), Cr1–O1 2.121(5); P1–Cr1–N1 92.15(16), P1–Cr1–Cl3 89.78(8), N1–Cr1–Cl3 87.09(15), N1–Cr1–Cl1 83.37(15), P1–Cr1–Cl2 88.80(8), O1–Cr1–Cl3 91.72(14).

octahedral geometry of Cr(III). A six-membered chelate is formed with the bidentate ligand 4, which occupies two coordination sites around chromium, binding through the nitrogen of the pyridine moiety and the phosphorus atom. Three chlorine atoms occupy three meridional coordination sites, while the last coordination site is occupied by one molecule of THF *trans* with respect to the phosphorus atom.

All bond lengths and bond angles are within the expected range.

As expected, variations in the bite angle and flexibility of the ancillary ligand do indeed affect the catalytic performance significantly (Table 2). Upon activation with MAO in toluene, 4a afforded a statistical distribution of oligomers with enrichment in C<sub>6</sub> and C<sub>8</sub> oligomers alongside significant amounts of PE (Table 2, entry 7). The C<sub>6</sub> and C<sub>8</sub> fraction existed of nearly pure 1-hexene and 1-octene (>99%). Methylcyclohexane as solvent led to a dramatic drop in activity as well as in purity of 1-hexene and 1-octene. Although 51% of the liquid products consisted of 1-octene (58% overall C<sub>8</sub> selectivity with an 88% purity of 1-octene), the production of oligomers is rather low compared with the solid (PE) fraction (Table 2, entry 8). Attempts to avoid PE formation by using a stronger reducing agent, triethylaluminum (TEA), indeed resulted in a decreased formation of unwanted polymer (Table 2, entry 10). However, a simultaneous decline in the selectivity for C<sub>6</sub> and C<sub>8</sub> was also observed. In a related Cr-aminophosphine system, a similar reduction of the PE formation has been reported, albeit that in this case the selectivity switched from C<sub>8</sub> toward C<sub>6</sub> while the overall C<sub>6</sub> and C<sub>8</sub> selectivity remained unchanged.<sup>18</sup> Similar to 1a, a higher ethylene pressure increased the catalytic activity of 4a, with only a slight influence on the product distribution (Table 2, entry 9). Although 4a produces a large amount of PE, over 50% of 1-octene selectivity for the liquid fraction indicates the existence of an active species for selective ethylene tetramerization, which is intriguing. To seek a highly selective ethylene tetramerization catalyst, ligand 4 was utilized in combination with more chromium precursors. The first attempt was to complex ligand 4 with methyl chromium dichloride, resulting in the microcrystalline green material 4b. Regrettably, the crystal shape of 4b was not suitable for undertaking a single crystal X-ray diffraction analysis. However, on the ground of elemental analytical and chemical degradation data, we propose a structure with the same octahedral geometry and group distribution as 4a. Complex 4b showed a similar trend as 4a: high activity for nonselective behavior in toluene and an increased selectivity for 1-hexene and 1-octene fractions when tested in methylcyclohexane. The activity of complex 4b was slightly higher than its trichloro analogue 4a, likely due to the

Scheme 5. Catalytic Behaviors of Ligands 1–6 in Combination with  $\text{CrCl}_3(\text{THF})_3$  upon Activation with MAO in Methylcyclohexane<sup>a</sup>



<sup>a</sup>The purity of 1-hexene and 1-octene is shown in parentheses. Activity in g/(mmol Cr·h).

increased solubility in aliphatic solvents as introduced to the Cr-alkyl function.

The catalytic behavior of **5a** is different from that of its closely related complexes **4a** and **2a**. When activated with MAO in toluene, complex **5a** produced polyethylene as the only product with moderate activity (Table 2, entry 11). In methylcyclohexane, PE was still the major product, but oligomers were formed as well (Table 2, entry 12). Complex **6a** showed promising catalytic behavior upon activation with MAO in methylcyclohexane (Table 2, entry 14). Despite the presence of PE, 1-hexene and 1-octene were obtained in very good purity and dominate the liquid fractions with an overall selectivity exceeding 98%. Toluene negatively affected the catalytic activity and selectivity (Table 2, entry 13). Besides a partial loss of  $\text{C}_6$  and  $\text{C}_8$  selectivity in the liquid phase, the productivity of oligomers in toluene also exhibits a significant drop compared with that in methylcyclohexane, which possibly arises from the formation of  $\text{Cr}(\text{I})-\eta^6\text{-toluene}$  complexes. The yield of PE was less affected by solvent, implying that PE is generated from chromium species with higher oxidation states.<sup>11,45–47</sup>

To avoid complications resulting from possible interaction between toluene and the  $\text{Cr}(\text{I})$  species, the catalytic outcomes of complexes **1a–6a** in methylcyclohexane were selected and summarized for further discussion. As it can be seen in Scheme 5, even a minor difference in the ligand structure can give rise to a noticeably different catalytic behavior. Introduction of a methylene bridge in the ligand backbone switches the selectivity of **1a** from 61% of  $\text{C}_6$  and 31% of  $\text{C}_8$  to 35% of  $\text{C}_6$  and 58% of  $\text{C}_8$  with a significant increase in the PE fraction for **4a**. By addition of one  $\text{CH}_2$  spacer between the pyridine and the aminophosphine fragments in **4a**, the resultant complex  $[\text{Py}(\text{CH}_2)_2\text{N}(\text{Me})\text{PPh}_2]\text{CrCl}_3\text{THF}$  (**Cr-PNPy**) has recently been reported to produce  $\text{C}_8$  with further enhanced selectivity of 75%.<sup>18</sup> Complexes **4a** and **Cr-PNPy** behave similarly in terms of activity. Furthermore, **1a** shows a much higher overall productivity as well as an improved oligomer/PE ratio than **4a**.

This observation indicates a possible correlation between the P–Cr–N bite angle and selectivity. In the case of the *o*-tolyl-substituted **2a** and **5a**, a similar trend in PE formation is observed with a larger bite angle and flexibility of the ligand resulting in an increased PE production. For **3a** and **6a**, containing more basic alkylphosphine moieties, the increased bite angle results in higher overall selectivity for 1-hexene and 1-octene, better purity of  $\alpha$ -olefin, and less PE. Variations of the ligand systems proved that for the phosphine substituents the P–Cr–N bite angle and ligand flexibility play a crucial role in controlling the catalytic performance of the catalysts.

## CONCLUSIONS

In the present study, chromium complexes bearing a series of pyridine–phosphine ligands have been synthesized and have shown varying catalytic behavior under typical reaction conditions for ethylene oligomerization.

The solvent choice has a pronounced influence on the catalytic activity as well as on the PE/oligomers ratio. The preference for aliphatic or aromatic surroundings is dependent on the ligand system. A possible reason could be that the interactions between solvent and active site are affected by the differences in steric bulk of the ancillary ligands, thereby leading to a shift in the equilibrium of active species responsible for ethylene oligomerization and polymerization. On the other hand, the selectivity of oligomer products is less affected by solvents.

Variations of the ligand structure have demonstrated that a dramatic change in catalytic behavior can be obtained upon a subtle modification in the ligand skeleton. For chromium complexes chelated by ligands **1–3**, steric bulk in the phosphine moiety plays a more pronounced role than the electronic effect in controlling catalytic activity, PE/oligomer ratio, and the purity of 1-hexene and 1-octene. Introduction of one  $\text{CH}_2$  unit between the pyridine and the aminophosphine moiety increases the flexibility of the ligand scaffold, resulting in a less distorted octahedral geometry with a P–Cr–N bite angle

close to 90°. According to the reaction conditions adopted, **4a**–**6a** enable nonselective oligomerization, selective tri- and tetramerization, and polymerization of ethylene. The diversity in catalytic outcomes of **4a**–**6a** might be attributed to the formation of various active species facilitated by chromium complexes bearing more flexible ligands **4**–**6**. Nevertheless, **6a** bearing the  $\text{PyCH}_2\text{N}(\text{Me})\text{P}^i\text{Pr}_2$  ligand shows potential for being a promising selective ethylene oligomerization catalyst, producing 1-hexene and 1-octene with high overall selectivity and very good purity, although thus far the formation of small amounts of PE is very persistent.

## EXPERIMENTAL SECTION

**General Procedures.** All manipulations for air or moisture sensitive materials were carried out under inert atmosphere in a glovebox or using Schlenk techniques. Dry solvents were obtained by passing them through a column purification system. Starting materials for ligand synthesis were purchased from Sigma-Aldrich and used as received. MAO (10 wt % in toluene solution) was purchased from Sigma-Aldrich and used as received. Dried MAO (DMAO) was prepared by pumping off all the volatile compounds of MAO at 40 °C for 6 h *in vacuo*, leaving a free-flowing white powder. All NMR spectra were recorded on Varian Mercury 400 or 500 MHz spectrometers at 25 °C.

**Ligand Synthesis.**  $\text{PyN}(\text{Me})\text{PPh}_2$  (**1**). A 2.5 M hexane solution of *n*-BuLi (10 mmol, 4 mL) was added dropwise to a stirred diethyl ether/petroleum ether (35 mL/20 mL) solution of 2-(methylamino)pyridine (10 mmol, 1.0 mL) at –78 °C. After 30 min of stirring, the reaction mixture was allowed to warm to room temperature and was stirred for additional 3 h.  $\text{PClPh}_2$  (10 mmol, 1.8 mL) was then added dropwise at 0 °C, and the reaction mixture was stirred overnight at room temperature. The resulting suspension was filtered and washed twice with diethyl ether (2 × 15 mL). The solvent was evaporated under reduced pressure until precipitation occurred. The supernatant was kept in the freezer (–30 °C), and the product was filtered and dried *in vacuo*, yielding a beige solid (2.4 g, 8 mmol, 80%).  $^1\text{H}$  NMR (400 MHz,  $\text{CD}_2\text{Cl}_2$ )  $\delta$ : 8.22 (d, 1H), 7.55 (t, 1H), 7.45–7.38 (m, 11H), 6.76 (t, 1H), 2.92 (d, 3H).  $^{31}\text{P}$  NMR (400 MHz,  $\text{CD}_2\text{Cl}_2$ )  $\delta$ : 50.82 (s).  $^{13}\text{C}$  NMR data were consistent with that reported in the literature.

$\text{PyN}(\text{Me})\text{P}(\text{o-tolyl})_2$  (**2**). Ligand **2** was synthesized similarly to ligand **1**, using chlorodi(*o*-tolyl)phosphine (2.49 g, 10 mmol). Recrystallization from diethyl ether/petroleum ether (10 mL/2 mL) gave colorless crystals (1.8 g, 5.6 mmol, 56%).  $^1\text{H}$  NMR (400 MHz,  $\text{CDCl}_3$ )  $\delta$ : 8.27 (d, 1H), 7.51 (t, 1H), 7.38–7.11 (m, 9H), 6.74 (t, 1H), 2.88 (d, 3H), 2.29 (s, 6H).  $^{31}\text{P}$  NMR (400 MHz,  $\text{CDCl}_3$ )  $\delta$ : 40.38 (s).  $^{13}\text{C}$  NMR (500 MHz,  $\text{CDCl}_3$ )  $\delta$ : 161.3, 147.7, 141.8, 137.0, 134.4, 130.7, 130.5, 129.1, 126.0, 114.4, 110.3, 34.7, 20.9.

$\text{PyN}(\text{Me})\text{P}^i\text{Pr}_2$  (**3**). Ligand **3** was synthesized similarly to ligand **1**, using chlorodiisopropylphosphine (1.6 mL, 10 mmol). After removal of the solvent *in vacuo*, the product was collected by distillation under reduced pressure (0.08 mbar, 50 °C) as a colorless oil (2.1 g, 9.2 mmol, 92%).  $^1\text{H}$  NMR (400 MHz,  $\text{CD}_2\text{Cl}_2$ )  $\delta$ : 8.14 (d, 1H), 7.44 (m, 2H), 6.64 (t, 1H), 3.06 (d, 3H), 2.18 (m, 2H), 1.16 (q, 6H), 1.03 (q, 6H).  $^{31}\text{P}$  NMR (400 MHz,  $\text{CD}_2\text{Cl}_2$ )  $\delta$ : 71.13 (s).  $^{13}\text{C}$  NMR (500 MHz,  $\text{CD}_2\text{Cl}_2$ )  $\delta$ : 147.0, 136.0, 113.3, 112.1, 111.0, 26.3, 19.2, 19.0.

$\text{PyCH}_2\text{N}(\text{Me})\text{PPh}_2$  (**4**). A 2.5 M hexane solution of *n*-BuLi (10 mmol, 4 mL) was added dropwise to a stirred diethyl ether solution (35 mL) of dipyrindyl amine (1.7 g, 10 mmol) at –78 °C. The formed yellow suspension was allowed to warm to room temperature and was stirred for another 2 h.  $\text{PPh}_2\text{Cl}$  (1.8 mL, 10 mmol) in diethyl ether (9 mL) was then added dropwise to the suspension at –78 °C. After stirring at –78 °C for 30 min, the suspension was slowly warmed to room temperature and stirred for 48 h. The suspension was filtered and washed with diethyl ether. The solvent of the filtrate was removed *in vacuo*, yielding a yellow solid. The solid was redissolved in petroleum ether (20 mL)/diethyl ether (5 mL), and the resulting orange suspension was filtered and washed with petroleum ether. The product

was dried *in vacuo*, yielding a white solid (2.3 g, 6.5 mmol, 65%).  $^1\text{H}$  NMR (400 MHz,  $\text{C}_6\text{D}_6$ )  $\delta$ : 8.14 (d, 2H), 7.70 (t, 4H), 6.99–6.92 (m, 6H), 6.55 (d, 2H), 6.29 (3, 2H).  $^{31}\text{P}$  NMR (400 MHz,  $\text{C}_6\text{D}_6$ )  $\delta$ : 52.03 (s).  $^{13}\text{C}$  NMR (500 MHz,  $\text{CDCl}_3$ )  $\delta$ : 160.1, 149.1, 139.1, 136.4, 132.2, 128.6, 128.3, 121.9, 62.5, 37.4.

$\text{PyCH}_2\text{N}(\text{Me})\text{P}(\text{o-tolyl})_2$  (**5**). Ligand **5** was synthesized similarly to ligand **1**, using methyl(2-pyridyl)methylamine (1.25 mL, 10 mmol) and chlorodi(*o*-tolyl)phosphine (2.49 g, 10 mmol). By evaporation of the solvent *in vacuo*, the product was collected as a red oil (3.0 g, 9 mmol, 90%).  $^1\text{H}$  NMR (400 MHz,  $\text{CDCl}_3$ )  $\delta$ : 8.52 (d, 1H), 7.60 (t, 1H), 7.28–7.12 (m, 10H), 4.44 (d, 2H), 2.51 (d, 3H), 2.36 (s, 6H).  $^{31}\text{P}$  NMR (400 MHz,  $\text{CDCl}_3$ )  $\delta$ : 55.48 (s).  $^{13}\text{C}$  NMR (500 MHz,  $\text{CDCl}_3$ )  $\delta$ : 160.3, 148.9, 141.2, 137.5, 136.4, 130.9, 130.3, 128.6, 125.8, 122.1, 63.6, 38.0, 21.1.

$\text{PyCH}_2\text{N}(\text{Me})\text{P}^i\text{Pr}_2$  (**6**). Ligand **6** was synthesized similarly to ligand **1**, using methyl(2-pyridyl)methylamine (1.25 mL, 10 mmol) and chlorodiisopropylphosphine (1.6 mL, 10 mmol). By evaporation of the solvent *in vacuo*, the product was collected as a brown oil (2.1 g, 8.8 mmol, 88%).  $^1\text{H}$  NMR (400 MHz,  $\text{CDCl}_3$ )  $\delta$ : 8.50 (d, 1H), 7.64 (t, 1H), 7.43 (d, 1H), 7.12 (t, 1H), 4.28 (d, 2H), 2.52 (d, 3H), 1.92 (m, 2H), 1.13–1.05 (m, 12 H).  $^{31}\text{P}$  NMR (400 MHz,  $\text{CDCl}_3$ )  $\delta$ : 89.99 (s).  $^{13}\text{C}$  NMR (500 MHz,  $\text{CDCl}_3$ )  $\delta$ : 160.6, 148.8, 136.3, 121.8, 64.1, 36.9, 26.7, 19.6, 19.2.

**Complex Synthesis.**  $[\text{PyN}(\text{Me})\text{PPh}_2]\text{CrCl}_3(\text{THF})$  (**1a**). A suspension of  $\text{CrCl}_3(\text{THF})_3$  (0.375 g, 1 mmol) in  $\text{CH}_2\text{Cl}_2$  (15 mL) was treated with ligand **1** (0.292 g, 1 mmol). The suspension was stirred overnight at room temperature. A small amount of insoluble material was removed by filtration, and the filtrate was evaporated *in vacuo*, affording **1a** as a pale blue powder (0.484 g, 0.93 mmol, 93%). Attempts to recrystallize **1a** from dichloromethane/petroleum ether resulted in microcrystalline material, unfortunately not suitable for a single X-ray diffraction analysis. Anal. Calcd (found) for  $\text{C}_{22}\text{H}_{25}\text{Cl}_3\text{CrN}_2\text{OP}$ : C 50.54 (50.94), H 4.82 (4.85), N 5.36 (5.38).

$[\text{PyN}(\text{Me})\text{P}(\text{o-tolyl})_2]\text{CrCl}_3(\text{THF})_2$  (**2a**). A suspension of  $\text{CrCl}_3(\text{THF})_3$  (0.188 g, 0.50 mmol) in THF (10 mL) was treated with ligand **2** (0.160 g, 0.50 mmol). The suspension was stirred overnight at room temperature. A small amount of insoluble material was removed by filtration, and the resulting solution was concentrated. Green crystals of **2a** (0.198 g, 0.36 mmol, 72%) were grown by vapor diffusion of petroleum ether into the THF solution at room temperature. Anal. calcd (found) for  $\text{C}_{24}\text{H}_{29}\text{Cl}_3\text{CrN}_2\text{OP}$ : C 53.99 (53.31), H 5.99 (6.00), N 4.50 (4.97).

$[\text{PyN}(\text{Me})\text{P}^i\text{Pr}_2]\text{CrCl}_3(\text{THF})$  (**3a**). A suspension of  $\text{CrCl}_3(\text{THF})_3$  (0.375 g, 1 mmol) in THF (15 mL) was treated with ligand **3** (0.224 g, 1 mmol). The suspension was stirred overnight at 50 °C. A small amount of insoluble material was removed by filtration, and the resulting solution was concentrated. Dark green crystals of **3a** (0.356 g, 0.78 mmol, 78%) were grown by vapor diffusion of petroleum ether into THF solution at room temperature. Anal. calcd (found) for  $\text{C}_{16}\text{H}_{29}\text{Cl}_3\text{CrN}_2\text{OP}$ : C 42.26 (42.26), H 6.43 (6.40), N 6.16 (6.15).

$[\text{PyCH}_2\text{N}(\text{Me})\text{PPh}_2]\text{CrCl}_3(\text{THF})$  (**4a**). A suspension of  $\text{CrCl}_3(\text{THF})_3$  (0.375 g, 1 mmol) in THF (15 mL) was treated with ligand **4** (0.306 g, 1 mmol). The suspension was stirred overnight at room temperature. A small amount of insoluble material was removed by filtration, and the resulting solution was concentrated and layered with petroleum ether affording **4a** at room temperature as dark green crystals (0.342 g, 0.64 mmol, 64%). Anal. Calcd (found) for  $\text{C}_{23}\text{H}_{27}\text{Cl}_3\text{CrN}_2\text{OP}$ : C 51.46 (50.86), H 5.07 (5.07), N 5.22 (5.15).

$[\text{PyCH}_2\text{N}(\text{Me})\text{PPh}_2]\text{MeCrCl}_2(\text{THF})$  (**4b**). A suspension of  $\text{MeCrCl}_2(\text{THF})_3$  (0.18 g, 0.5 mmol) in toluene (5 mL) was treated with ligand **4** (0.15 g, 0.5 mmol). The suspension turned dark green immediately, and stirring was continued for additional 12 h. The insoluble complex was collected by centrifugation and redissolved in THF (5 mL). The olive green solution was layered with heptane (2 mL). The formed crystalline mass was washed with cold hexane (2 × 2 mL) and dried *in vacuo* (0.19 g, 0.37 mmol, 74%). Anal. calcd (found) for  $\text{C}_{24}\text{H}_{30}\text{Cl}_2\text{CrN}_2\text{OP}$ : C 41.68 (41.44), H 5.95 (5.87), N 9.72 (9.66).

$[\text{PyCH}_2\text{N}(\text{Me})\text{P}(\text{o-tolyl})_2]\text{CrCl}_3(\text{THF})$  (**5a**). A suspension of  $\text{CrCl}_3(\text{THF})_3$  (0.375 g, 1 mmol) in THF (15 mL) was treated with ligand **5** (0.334 g, 1 mmol). The suspension was stirred overnight at 50

°C. A small amount of insoluble material was removed by filtration, and the filtrate was dried *in vacuo*, affording **5a** as a green powder (0.318 g, 0.56 mmol, 56%). Anal. calcd (found) for  $C_{25}H_{31}Cl_3CrN_2OP$ : C 53.16 (54.43), H 5.53 (5.83), N 4.96 (5.49).

**[PyCH<sub>2</sub>N(Me)P'Pr<sub>2</sub>]CrCl<sub>3</sub>(THF) (6a)**. A suspension of  $CrCl_3(THF)_3$  (0.375 g, 1 mmol) in THF (15 mL) was treated with ligand **6** (0.238 g, 1 mmol). The suspension was stirred overnight at room temperature. A small amount of insoluble material was removed by filtration, and the filtrate was dried *in vacuo*, affording **6a** as green powder (0.401 g, 0.86 mmol, 86%). Anal. calcd (found) for  $C_{17}H_{31}Cl_3CrN_2OP$ : C 43.56 (42.15), H 6.67 (6.86), N 5.98 (5.05).

**Ethylene Oligomerization.** All of the ethylene oligomerization experiments were performed in a 200 mL steel Büchi autoclave. The autoclave was heated in an oven overnight at 150 °C before each run. After evacuation and rinsing with argon three times, the solvent (volume of solvent = total volume (100 mL) – volume of catalyst solution – volume of cocatalyst solution) was charged in the preheated autoclave. Then cocatalyst was injected, and the solvent was saturated with ethylene by pressurizing to 30 bar. After 30 min of stirring, the autoclave was temporarily vented to allow the injection of the catalyst solution. The autoclave was repressurized to the desired pressure, and the pressure was maintained throughout the run. The temperature of the autoclave was controlled by a thermostat bath. After 30 min, the reaction was quenched by cooling to 0 °C, depressurizing, and injection of a mixture of ethanol and diluted hydrochloric acid. The polymer was separated by filtration and dried overnight at 60 °C under reduced pressure before mass determination. The oligomers were analyzed by GC-FID for oligomer composition and by <sup>1</sup>H NMR spectroscopy for activity.

**X-ray Crystallography.** Data collection results for compounds **2a** and **4a** represent the best data sets obtained in several trials for each sample. The crystals were mounted on thin glass fibers using paraffin oil. Prior to data collection, crystals were cooled to 200.15 K. Data were collected on a Bruker AXS KAPPA single crystal diffractometer equipped with a sealed Mo tube source (wavelength 0.71073 Å) APEX II CCD detector. Raw data collection and processing were performed with APEX II software package from BRUKER AXS.<sup>48</sup> Diffraction data for **2a** and **4a** samples were collected with a sequence of 0.5°  $\omega$  scans at 0, 120°, and 240° in  $\varphi$ . Initial unit cell parameters were determined from 60 data frames with 0.3°  $\omega$  scan each, collected at the different sections of the Ewald sphere. Semiempirical absorption corrections based on equivalent reflections were applied.<sup>49</sup> Systematic absences in the diffraction data set and unit-cell parameters were consistent with monoclinic  $P2_1/n$  (No. 14, alternative settings) for compound **2a** and orthorhombic  $P2_12_12_1$  (No. 19) for **4a**. Solutions in the centrosymmetric space group for **2a** compound yielded chemically reasonable and computationally stable results of refinement. However, data for the complex **4a** suggested noncentrosymmetric space group for the structural solution and model refinement. The structures were solved by direct methods, completed with difference Fourier synthesis, and refined with full-matrix least-squares procedures based on  $F^2$ .

Diffraction data for the crystal of the complex **2a** were collected to 0.75 Å resolution; however due to small crystal size and weak diffraction it was discovered that both  $R(\text{int})$  and  $R(\sigma)$  exceed 35% for the data below 1.00 Å resolution. Based on  $R(\sigma)$  value, data were truncated to 0.95 Å resolution for refinement. Asymmetric unit for this crystallographic model of **2a** consists of one target complex molecule and one THF crystallization solvent molecule. Both molecules are located in the general positions. Occupancy of atomic positions for THF solvent molecules was initially allowed to refine in order to achieve acceptable values for thermal motion parameters. After initial refinement, occupancy of THF molecule was restrained at 50%. All non-hydrogen atoms in the structure were refined anisotropically.

Asymmetric unit of **4a** contains one chiral compound molecule and one THF solvent molecule. Both parts of the structural model are located in the general positions. Location of strong residual electron density peak next to oxygen atom of the THF molecule suggested oxygen positional disorder. Atomic position was split in two, and occupancies of the both positions were restrained to 50%, providing acceptable values of thermal motion parameters. Initially the attempt

was made to refine THF solvent molecule atomic positions with anisotropic displacement coefficients. However, this attempt required introduction of significant amount of displacement and geometry constrains. For that reason THF molecule was refined with isotropic thermal displacement parameters set. All non-hydrogen atoms of the target compound were refined anisotropically. Final Flack parameter value due to chiral space group was refined to  $-0.015(18)$ .

For all the compounds, all hydrogen atoms positions were calculated based on the geometry of bearing non-hydrogen atoms. All hydrogen atoms were treated as idealized contributions during the refinement. All scattering factors are contained in several versions of the SHELXTL program library, with the latest version used being v.6.12.<sup>50</sup> Crystallographic data and selected data collection parameters are reported in Tables 1.

## ■ ASSOCIATED CONTENT

### 📄 Supporting Information

Crystallographic data for **2a** and **4a** in CIF format. This material is available free of charge via the Internet at <http://pubs.acs.org>.

## ■ AUTHOR INFORMATION

### Corresponding Authors

\*E-mail: [r.duchateau@tue.nl](mailto:r.duchateau@tue.nl) (Robbert Duchateau).

\*E-mail: [sgambaro@uottawa.ca](mailto:sgambaro@uottawa.ca). (Sandro Gambarotta).

### Notes

The authors declare no competing financial interest.

## ■ ACKNOWLEDGMENTS

We'd like to thank the Chinese Scholarship Council, the Natural Science Foundation of China (No. 21004020 and No. 21174037), and the Eindhoven University of Technology for financial support.

## ■ REFERENCES

- (1) Dixon, J. T.; Green, M. J.; Hess, F. M.; Morgan, D. H. *J. Organomet. Chem.* **2004**, *689*, 3641–3668.
- (2) Wass, D. F. *Dalton Trans.* **2007**, *2007*, 816–819.
- (3) Agapie, T. *Coord. Chem. Rev.* **2011**, *255*, 861–880.
- (4) McGuinness, D. S. *Chem. Rev.* **2011**, *111*, 2321–2341.
- (5) van Leeuwen, P. W. N. M.; Clément, N. D.; Tschan, M. J. L. *Coord. Chem. Rev.* **2011**, *255*, 1499–1517.
- (6) Bryliakov, K. P.; Talsi, E. P. *Coord. Chem. Rev.* **2012**, *256*, 2994–3007.
- (7) McGuinness, D. S.; Wasserscheid, P.; Keim, W.; Hu, C.; Englert, U.; Dixon, J. T.; Grove, C. *Chem. Commun.* **2003**, *3*, 334–335.
- (8) Carter, A.; Cohen, S. A.; Cooley, N. A.; Murphy, A.; Scutt, J.; Wass, D. F. *Chem. Commun.* **2002**, *2002*, 858–859.
- (9) Bollmann, A.; Blann, K.; Dixon John, T.; Hess Fiona, M.; Killian, E.; Maumela, H.; McGuinness David, S.; Morgan David, H.; Neveling, A.; Otto, S.; Overett, M.; Slawin Alexandra, M. Z.; Wasserscheid, P.; Kuhlmann, S. *J. Am. Chem. Soc.* **2004**, *126*, 14712–14713.
- (10) Peitz, S.; Peulecke, N.; Aluri, B. R.; Hansen, S.; Müller, B. H.; Spannenberg, A.; Rosenthal, U.; Al-Hazmi, M. H.; Mosa, F. M.; Wöhl, A.; Müller, W. *Eur. J. Inorg. Chem.* **2010**, *2010*, 1167–1171.
- (11) Albahily, K.; Koc, E.; Al-Baldawi, D.; Savard, D.; Gambarotta, S.; Burchell, T. J.; Duchateau, R. *Angew. Chem., Int. Ed.* **2008**, *47*, 5816–5819.
- (12) Thapa, I.; Gambarotta, S.; Korobkov, I.; Duchateau, R.; Kulangara, S. V.; Chevalier, R. *Organometallics* **2010**, *29*, 4080–4089.
- (13) Albahily, K.; Fomitcheva, V.; Gambarotta, S.; Korobkov, I.; Murugesu, M.; Gorelsky, S. I. *J. Am. Chem. Soc.* **2011**, *133*, 6380–6387.
- (14) Albahily, K.; Fomitcheva, V.; Shaikh, Y.; Sebastiao, E.; Gorelsky, S. I.; Gambarotta, S.; Korobkov, I.; Duchateau, R. *Organometallics* **2011**, *30*, 4201–4210.

- (15) Albahily, K.; Shaikh, Y.; Sebastiao, E.; Gambarotta, S.; Korobkov, I.; Gorelsky, S. I. *J. Am. Chem. Soc.* **2011**, *133*, 6388–6395.
- (16) Thapa, I.; Gambarotta, S.; Korobkov, I.; Murugesu, M.; Budzelaar, P. *Organometallics* **2011**, *31*, 486–494.
- (17) Shaikh, Y.; Albahily, K.; Sutcliffe, M.; Fomitcheva, V.; Gambarotta, S.; Korobkov, I.; Duchateau, R. *Angew. Chem., Int. Ed.* **2012**, *51*, 1366–1369.
- (18) Shaikh, Y.; Gurnham, J.; Albahily, K.; Gambarotta, S.; Korobkov, I. *Organometallics* **2012**, *31*, 7427–7433.
- (19) Klemps, C.; Payet, E.; Magna, L.; Saussine, L.; Le Goff, X. F.; Le Floch, P. *Chem.—Eur. J.* **2009**, *15*, 8259–8268.
- (20) Bowen, L. E.; Haddow, M. F.; Orpen, A. G.; Wass, D. F. *Dalton Trans.* **2007**, *2007*, 1160–1168.
- (21) Dulai, A.; McMullin, C. L.; Tenza, K.; Wass, D. F. *Organometallics* **2011**, *30*, 935–941.
- (22) Stennett, T. E.; Haddow, M. F.; Wass, D. F. *Organometallics* **2012**, *31*, 6960–6965.
- (23) Sydora, O. L.; Jones, T. C.; Small, B. L.; Nett, A. J.; Fischer, A. A.; Carney, M. J. *ACS Catal.* **2012**, *2*, 2452–2455.
- (24) Agapie, T.; Day, M. W.; Henling, L. M.; Labinger, J. A.; Bercaw, J. E. *Organometallics* **2006**, *25*, 2733–2742.
- (25) Schofer, S. J.; Day, M. W.; Henling, L. M.; Labinger, J. A.; Bercaw, J. E. *Organometallics* **2006**, *25*, 2743–2749.
- (26) Elowe, P. R.; McCann, C.; Pringle, P. G.; Spitzmesser, S. K.; Bercaw, J. E. *Organometallics* **2006**, *25*, 5255–5260.
- (27) Blann, K.; Bollmann, A.; de Bod, H.; Dixon, J. T.; Killian, E.; Nongodlwana, P.; Maumela, M. C.; Maumela, H.; McConnell, A. E.; Morgan, D. H.; Overett, M. J.; Pretorius, M.; Kuhlmann, S.; Wasserscheid, P. *J. Catal.* **2007**, *249*, 244–249.
- (28) Mao, G.; Ning, Y.; Hu, W.; Li, S.; Song, X.; Niu, B.; Jiang, T. *Chin. Sci. Bull.* **2008**, *53*, 3511–3515.
- (29) Peitz, S.; Peulecke, N.; Aluri, B. R.; Müller, B. H.; Spannenberg, A.; Rosenthal, U.; Al-Hazmi, M. H.; Mosa, F. M.; Wöhl, A.; Müller, W. *Organometallics* **2010**, *29*, 5263–5268.
- (30) Reddy Aluri, B.; Peulecke, N.; Peitz, S.; Spannenberg, A.; Müller, B. H.; Schulz, S.; Drexler, H.-J.; Heller, D.; Al-Hazmi, M. H.; Mosa, F. M.; Wöhl, A.; Müller, W.; Rosenthal, U. *Dalton Trans.* **2010**, *39*, 7911–7920.
- (31) Peitz, S.; Peulecke, N.; Müller, B. H.; Spannenberg, A.; Drexler, H. J.; Rosenthal, U.; Al-Hazmi, M. H.; Al-Eidan, K. E.; Wöhl, A.; Müller, W. *Organometallics* **2011**, *30*, 2364–2370.
- (32) Müller, B. H.; Peulecke, N.; Spannenberg, A.; Rosenthal, U.; Al-Hazmi, M. H.; Schmidt, R.; Wöhl, A.; Müller, W. *Organometallics* **2012**, *31*, 3695–3699.
- (33) Licciulli, S.; Thapa, I.; Albahily, K.; Korobkov, I.; Gambarotta, S.; Duchateau, R.; Chevalier, R.; Schuhen, K. *Angew. Chem., Int. Ed.* **2010**, *49*, 9225–9228.
- (34) Blann, K.; Bollmann, A.; Dixon, J. T.; Hess, F. M.; Killian, E.; Maumela, H.; Morgan, D. H.; Neveling, A.; Otto, S.; Overett, M. J. *Chem. Commun.* **2005**, *2005*, 620–621.
- (35) Overett, M. J.; Blann, K.; Bollmann, A.; Dixon, J. T.; Hess, F.; Killian, E.; Maumela, H.; Morgan, D. H.; Neveling, A.; Otto, S. *Chem. Commun.* **2005**, *2005*, 622–624.
- (36) Crewdson, P.; Gambarotta, S.; Djoman, M. C.; Korobkov, I.; Duchateau, R. *Organometallics* **2005**, *24*, 5214–5216.
- (37) Vidyaratne, I.; Nikiforov, G. B.; Gorelsky, S. I.; Gambarotta, S.; Duchateau, R.; Korobkov, I. *Angew. Chem., Int. Ed.* **2009**, *48*, 6552–6556.
- (38) Overett, M. J.; Blann, K.; Bollmann, A.; Dixon, J. T.; Haasbroek, D.; Killian, E.; Maumela, H.; McGuinness, D. S.; Morgan, D. H. *J. Am. Chem. Soc.* **2005**, *127*, 10723–10730.
- (39) Budzelaar, P. H. M. *Can. J. Chem.* **2009**, *87*, 832–837.
- (40) Calucci, L.; Englert, U.; Grigiotti, E.; Laschi, F.; Pampaloni, G.; Pinzino, C.; Volpe, M.; Zanello, P. *J. Organomet. Chem.* **2006**, *691*, 829–836.
- (41) Walsh, R.; Morgan, D. H.; Bollmann, A.; Dixon, J. T. *Appl. Catal., A* **2006**, *306*, 184–191.
- (42) Kuhlmann, S.; Paetz, C.; Hagele, C.; Blann, K.; Walsh, R.; Dixon, J. T.; Scholz, J.; Haumann, M.; Wasserscheid, P. *J. Catal.* **2009**, *262*, 83–91.
- (43) Chen, E. Y.-X.; Marks, T. J. *Chem. Rev.* **2000**, *100*, 1391–1434.
- (44) McGuinness, D. S.; Suttill, J. A.; Gardiner, M. G.; Davies, N. W. *Organometallics* **2008**, *27*, 4238–4247.
- (45) Albahily, K.; Ahmed, Z.; Gambarotta, S.; Koç, E.; Duchateau, R.; Korobkov, I. *Organometallics* **2011**, *30*, 6022–6027.
- (46) Jabri, A.; Mason, C. B.; Sim, Y.; Gambarotta, S.; Burchell, T. J.; Duchateau, R. *Angew. Chem., Int. Ed.* **2008**, *47*, 9717–9721.
- (47) Albahily, K.; Al-Baldawi, D.; Gambarotta, S.; Koc, E.; Duchateau, R. *Organometallics* **2008**, *27*, 5943–5947.
- (48) APEX Software Suite v.2012; Bruker AXS: Madison, WI, 2005.
- (49) Blessing, R. *Acta Crystallogr.* **1995**, *A51*, 33.
- (50) Sheldrick, G. M. *Acta Crystallogr.* **2008**, *A64*, 112.